Liquid Crystals
Publication details, including instructions for authors and subscription information:
http://www.informaworld.com/smpp/title~content=t713926090

Polymer network structure and electro-optic performance of polymer stabilized cholesteric textures I. The influence of curing temperature

I. Dierking; L. L. Kosbar; A. C. Lowe; G. A. Held

To cite this Article Dierking, I. , Kosbar, L. L. , Lowe, A. C. and Held, G. A.(1998) 'Polymer network structure and electro-optic performance of polymer stabilized cholesteric textures I. The influence of curing temperature', Liquid Crystals, 24: 3, 387 — 395

To link to this Article: DOI: 10.1080/026782998207208

URL: http://dx.doi.org/10.1080/026782998207208

LIQUID CRYSTALS, 1998, VOL. 24, NO. 3, 387–395

Polymer network structure and electro-optic performance of polymer stabilized cholesteric textures
I. The influence of curing temperature

by I. DIERKING†, L. L. KOSBAR, A. C. LOWE and G. A. HELD*
IBM T.J. Watson Research Center, P.O. Box 218, Yorktown Heights, NY 10598, USA

(*Received 18 July 1997; accepted 8 September 1997*)

The effect of curing temperature on the electro-optic behaviour and network morphology of reverse mode polymer stabilized cholesteric textures (PSCTs) has been studied. Scanning electron micrographs indicate that increasing the curing temperature generally results in a larger average void size within a polymer network, while the morphology of the individual strands (which varies significantly for different monomers) remains largely unchanged. PSCTs with sufficiently large network voids exhibit a two-stage switching behaviour consistent with a model in which the cholesteric liquid crystal is divided between two distinct environments—one in which the liquid crystal is strongly dominated by the polymer network, the other in which a bulk-like behaviour, comparable to the unstabilized cholesteric material, is observed.

1. Introduction

Polymer stabilized liquid crystals are of interest both for their applicability to display devices and for the fundamental insights they offer on liquid crystal/polymer composites [1, 2]. One such system which in recent years has attracted wide interest is the *reverse mode* polymer stabilized cholesteric texture (PSCT) [3, 4]. At zero field, a cholesteric with a pitch in the infrared (typically several μm) is oriented in the planar Grandjean texture, which is then stabilized by the formation of a polymer network within the liquid crystal material. This planar state appears transparent and exhibits very low reflectivity for visible light. Application of an electric field in the direction of the helical axis results in a reorientation of the liquid crystal into the focal-conic configuration, a state which is strongly scattering and which exhibits high reflectivity. In this system, the polymer network serves two important functions. First, it influences the structure of the focal-conic state, and thus greatly influences the scattering properties of the system. Second, following the removal of the electric field, elastic forces between the polymer network and the liquid crystal cause a rapid reorientation back to the planar, non-scattering texture.

Recently, we have reported that the transition between the planar and focal-conic states of a reverse mode PSCT device may occur via either a one- or a two-stage switching process [5], dependent upon the composition and concentration of the polymer network. We utilized SEM to characterize the morphologies of the various networks and, comparing SEM and electro-optical data, concluded that the observed two-stage switching resulted from the cholesteric liquid crystal being divided between two distinct environments. In the first, the liquid crystal is strongly dominated by the polymer network, while in the second a bulk-like behaviour, comparable to the unstabilized cholesteric material, is observed. Depending on the choice of monomer, the resulting polymer network was either a finely stranded and highly interconnected network or a coarse network composed of micron size 'rice-grain-like' particles. For the finely stranded polymers, the presence of large voids in the network (which accounted for the two-stage switching) appeared only at low monomer concentrations, whereas for the coarser networks these voids were present at all concentrations studied.

To understand more fully the processes which determine polymer morphology of PSCT systems, we have carried out a detailed study of the dependence of both polymer structure and electro-optical properties on polymer curing temperature. We find that curing temperature does indeed affect the average size of the voids within a network. For both of the monomers studied, increasing the temperature had the effect of increasing the average void size within the network. This resulted in changes in the reflectivity and transmittance consistent with our

---

† Present address: Liquid Crystal Group, Physics Department, Chalmers University of Technology, S-41296 Göteborg, Sweden.

*Author for correspondence.

0267–8292/98 $12·00 © 1998 Taylor & Francis Ltd.

earlier model [5]. Further, for the case of the finely stranded RM206 polymer network, increasing the curing temperature resulted in a transition from one- to two-stage switching—again consistent with increasingly large voids in the network. However, the qualitative structure of the networks was not significantly altered by varying the curing temperature, suggesting that there are other important factors which influence the polymer growth and final morphology.

2. Experimental methods

The nematic matrix used in this study was the mixture E48 (Merck Industries), doped with 0·5 wt % of the chiral agent R1011 (Merck Industries), to produce an induced cholesteric with a pitch of 10 μm. The phase behaviour of the E48/R1011 mixture, as determined by differential scanning calorimetry (DSC), is given by: Cr −19 N* 87 I. For each cell, a mesogenic reactive monomer (either RM206† or BMBB-6 [4]) was dissolved in the chiral nematic liquid crystal at 6 wt %. A small amount (2 wt %) of benzoin methyl ether (BME) was added to the monomer to act as a photoinitiator. Addition of the reactive monomers to the liquid crystal caused a depression of the clearing temperature by a few degrees. The liquid crystal–monomer solutions were vacuum filled into 15-μm-thick cells with low pretilt, anti-parallel rubbed polyimide alignment layers, where the cell thickness was controlled by a dispersion of cylindrical spacer beads. The cells were sealed and irradiated by a UV source at 0·5 mW cm^{-2} for 5·5 h, with the liquid crystal in the planar orientation. Thus, the resulting polymer network structure was expected to follow the local helical order of the liquid crystal. The temperature during curing was controlled with an accuracy of ±1°C and the range of curing temperatures studied was from −10 to 60°C. The lower limit was set by the crystallization temperature of the cholesteric, while the upper temperature was limited by a reduction in the order parameter. Samples prepared above 60°C exhibited non-reproducible electro-optic behaviour.

The diffuse reflectivity (fraction of back scattered light) and the diffuse transmittance (fraction of forward scattered light) were measured on an absolute scale using an integrating sphere (Oriel Instruments). Texture transitions were induced by a sine wave voltage of frequency $f = 2$–5 kHz at variable amplitude, and the sample was illuminated with a 633 nm HeNe laser. Depending on the detection method employed, either the static or dynamic response of the cell was measured [5]. For dynamic measurements the electric field amplitude was chosen to ensure a saturated switching process and response times were evaluated for a 10–90% change in scattered light intensity.

Scanning electron microscope investigations (Hitachi S-800 SEM) of the polymer networks were carried out following removal of the liquid crystal from the samples. To ensure that the polymer network was not altered during the preparation process, the following novel sample preparation procedure was developed. Opposite edges of the cell were ground off and the liquid crystal removed by immersion of the cell in a suitable solvent (diethyl ether). The solvent was in turn replaced with liquid CO_2, which was then brought continuously (i.e. without going through a first-order vaporization transition) into the gaseous state [6]. Following this, the cell was filled with a reworkable epoxy which was then thermally cured. Part of the cell was then ground away to expose the polymer, ensconced within the epoxy. Finally, a thin layer of the epoxy was dissolved away in a dilute acid to expose the unsupported polymer network. The surface was metallized and subjected to SEM analysis. We note that only when this procedure was followed were we able to resolve a helical structure within high (>5 wt %) polymer content RM206 networks [5]. We take this as evidence that this procedure does not significantly disrupt the PSCT network structure.

3. Experimental results

3.1. *Diffuse reflectivity*

The experimentally determined diffuse reflectivity, measured for different curing temperatures, is shown in figure 1 (*a*) and (*b*) for RM206 and BMBB-6 based samples, respectively. All of the BMBB-6 samples studied exhibit a two-stage switching process similar to that reported previously. In contrast, only those RM206 samples which were cured above 35°C exhibit two-stage switching, and even in these cases the two-stage switching is less pronounced than that observed in the BMBB-6 data. The two reorientation processes in RM206 samples cured at high temperatures (as well as the single stage reorientation process in samples cured at low temperatures) can be observed more clearly in time resolved measurements of the diffuse reflectivity (figure 2). When the electric field is removed at $t = 50$ ms, the diffuse reflectivity reveals the dynamics of the transition from the focal-conic to the planar state. For the sample cured at 51°C (diamonds), a fast reorientation is followed by a second, much slower process, whereas for the sample cured at 14°C (circles), only a single, fast reorientation process can be observed. Maximum diffuse reflectivity is found, in general, to decrease with increasing curing temperature (figure 3). Similarly, the threshold voltage for the onset of diffuse reflectivity decreases with increasing curing temperature (figure 4).

PSCT cells have two distinct dynamic responses—one

---

† RM206 is a mesogenic diacrylate whose exact structure is proprietary to Merck Industries.

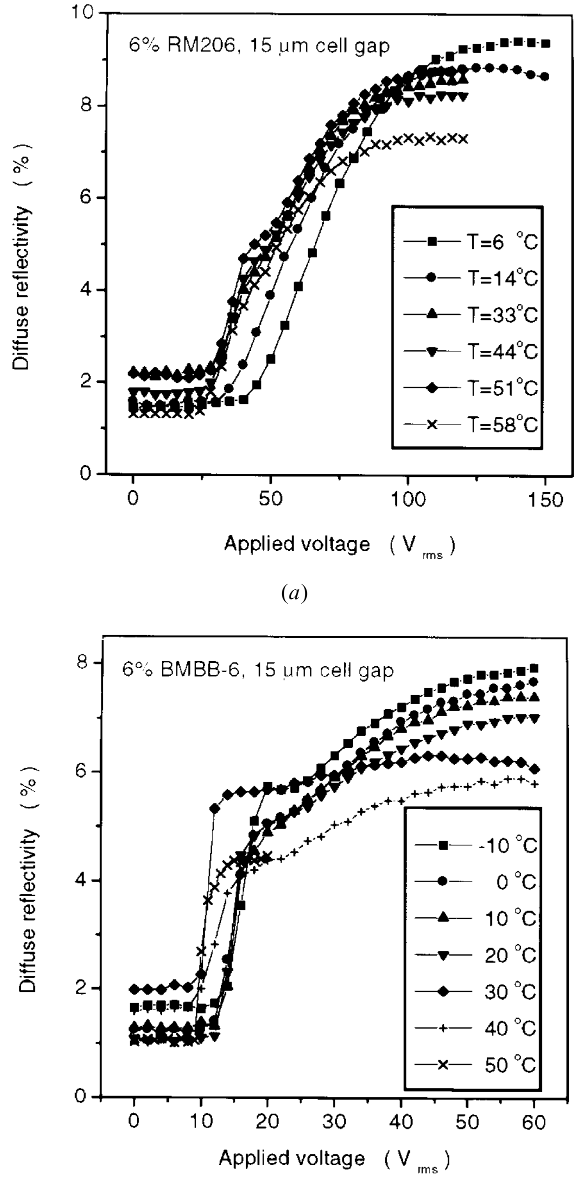

(*a*)

(*b*)

Figure 1. Diffuse reflectivity (fraction of back scattered light) as a function of applied voltage for various curing temperatures for (*a*) 6 wt % RM206 and (*b*) 6 wt % BMBB-6 polymer stabilized samples.

for the transition from the planar to the focal-conic state (the rise time) and the other for the switching from the field-induced, scattering focal-conic state back to the planar, non-scattering texture at zero field (the decay time). The former reorientation process is dependent on the applied electric field amplitude, as dielectric interactions are driving this transition. Thus, rise times can be compared only if the same voltage can be applied to all of the samples. For this reason, all dynamic response measurements of the RM206 samples were taken with

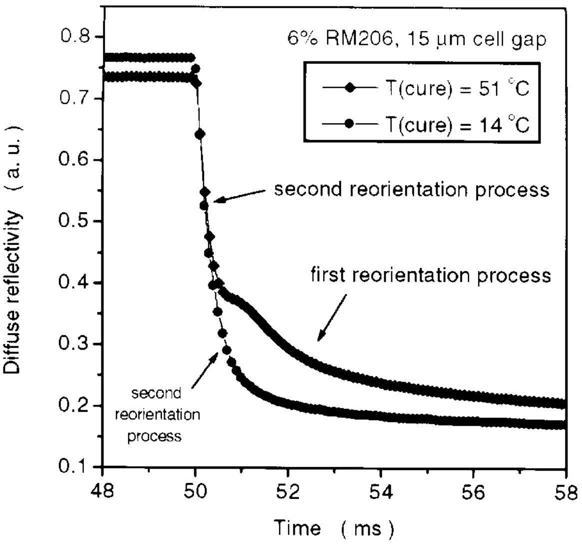

Figure 2. Dynamic response of the diffuse reflectivity of 6 wt % RM206 samples. These data show the reorientation from the focal-conic to the planar state following the removal of the applied field at $t=50$ ms. For high curing temperatures (51°C) a two-stage switching is observed, whereas only a single-stage reorientation is observed for low curing temperatures (14°C).

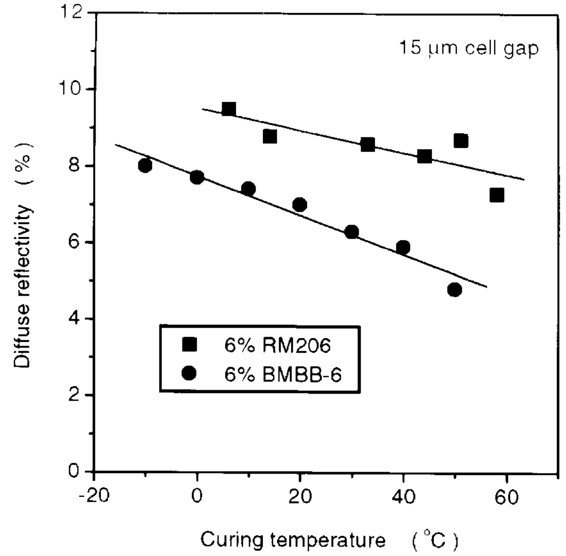

Figure 3. Dependence of the maximum observed diffuse reflectivity on curing temperature for 6 wt % RM206 (■) and 6 wt % BMBB-6 (●) polymer networks.

driving voltages of 120 V rms. For the BMBB-6 samples, the dynamic response of the diffuse reflectivity was measured for an applied voltage of 60 V rms, whereas the diffuse transmittance was measured with an applied voltage of 25 V rms. The relaxation process following removal of the applied field is basically governed by elastic forces between the polymer network and the

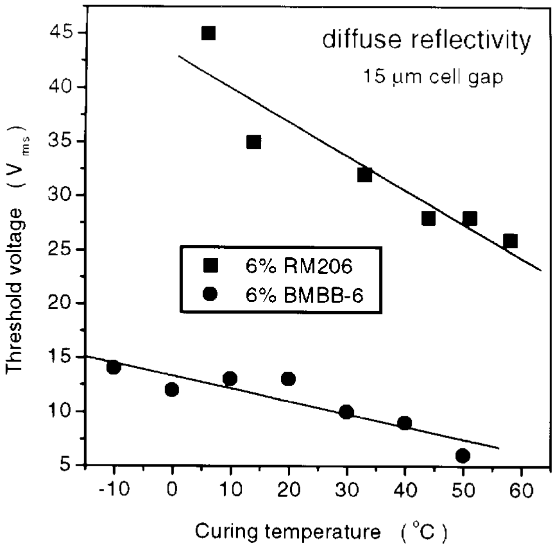

Figure 4. Dependence of the threshold voltage of the diffuse reflectivity on curing temperature for the planar to focal-conic texture transition for 6 wt % RM206 (■) and 6 wt % BMBB-6 (●) polymer networks.

liquid crystal; thus the decay times can, to first approximation, be considered as electric field independent. Rise times of the diffuse reflectivity of RM206 and BMBB-6 [figure 5 (*a*) and (*b*), closed symbols] are found to be independent of the curing temperature. This suggests that lowering the curing temperature does not result in an increase in the concentration of oligomers remaining in the liquid crystal, as this would increase the viscosity which, in turn, would increase the rise times. The decay times, however, do increase with increasing curing temperature [figure 5 (*a*) and (*b*), open symbols]. This suggests that as the curing temperature increases, the polymer network plays a less dominant role in the reorientation process.

3.2. *Diffuse transmittance*

The experimentally determined diffuse transmittance, measured for different curing temperatures, is shown in figure 6 (*a*) and (*b*) for RM206 and BMBB-6 based samples, respectively. As is apparent from these data, no two-stage switching can be detected for the diffuse transmittance; the director reorientation from planar to focal-conic is observed as a steep increase in the diffuse transmittance over a rather narrow voltage regime. The decrease in diffuse transmittance, which can be observed for some of the samples as the voltage is further increased, is due to a partial transition into the homeotropic configuration. Generally, we observe an increase in the diffuse transmittance (forward scattering) with increasing curing temperature, although this trend is clearly pronounced only for the RM206 data (figure 7).

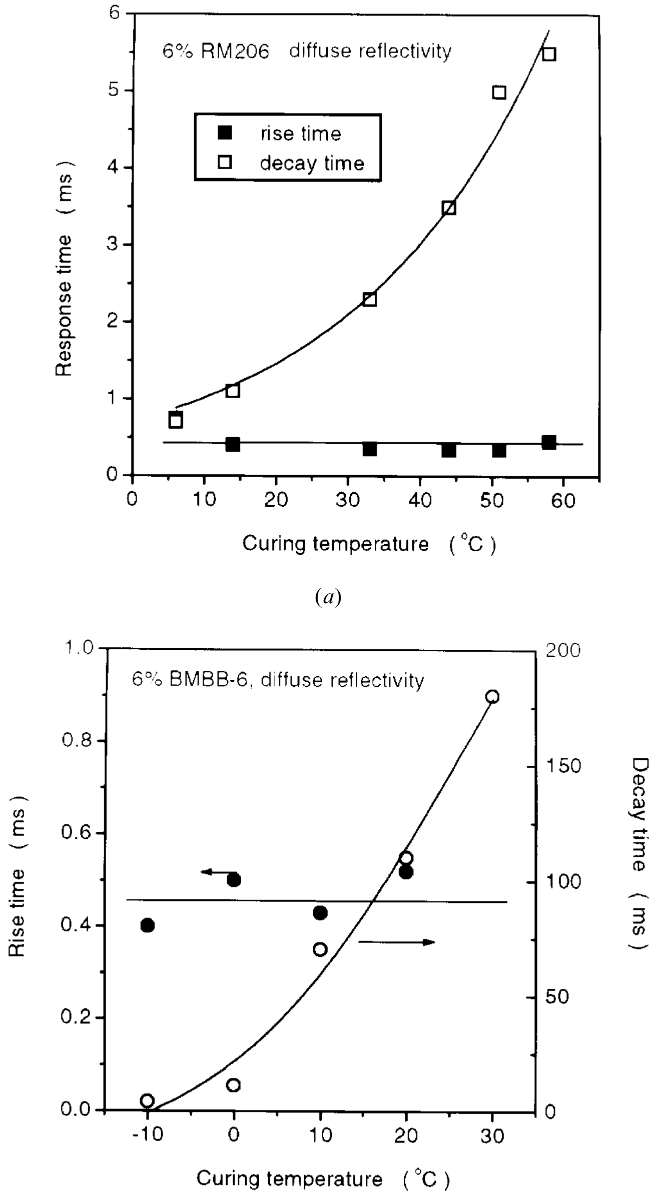

(*a*)

(*b*)

Figure 5. Dependence of the response times of the diffuse reflectivity on curing temperature for the planar to focal-conic texture transition for (*a*) 6 wt % RM206 (■) and (*b*) 6 wt % BMBB-6 (●) polymer networks. Rise times are shown with closed symbols and decay times with open symbols.

Also, the threshold voltage of the onset of diffuse transmittance decreases as the curing temperature is increased (figure 8).

As with the diffuse reflectivity, the rise times observed from the dynamic response of the diffuse transmittance for both RM206 and BMBB-6 are independent of the curing temperature [figure 9 (*a*) and (*b*), closed symbols]. Also in agreement with the diffuse reflectivity, the decay

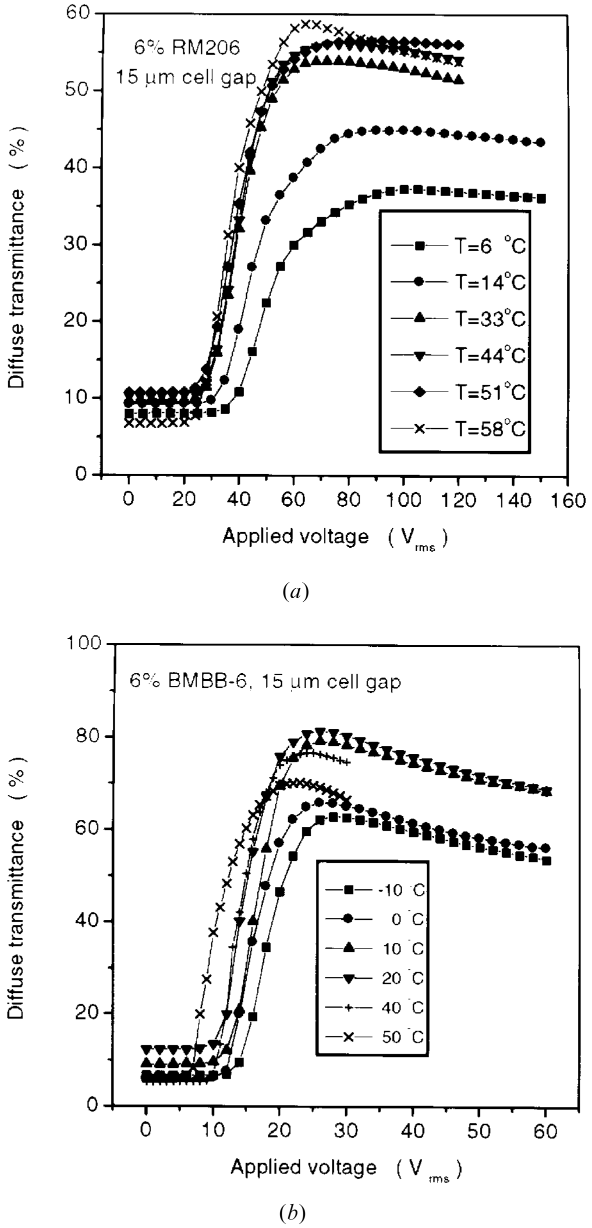

(*a*)

(*b*)

Figure 6. Diffuse transmittance (fraction of forward scattered light) as a function of applied voltage for various curing temperatures for (*a*) 6 wt % RM206 and (*b*) 6 wt % BMBB-6 polymer stabilized samples.

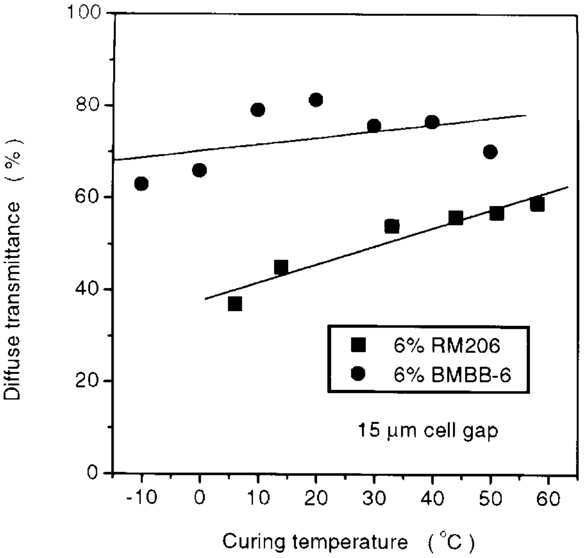

Figure 7. Dependence of the maximum observed diffuse transmittance on curing temperature for 6 wt % RM206 (■) and 6 wt % BMBB-6 (●) polymer networks.

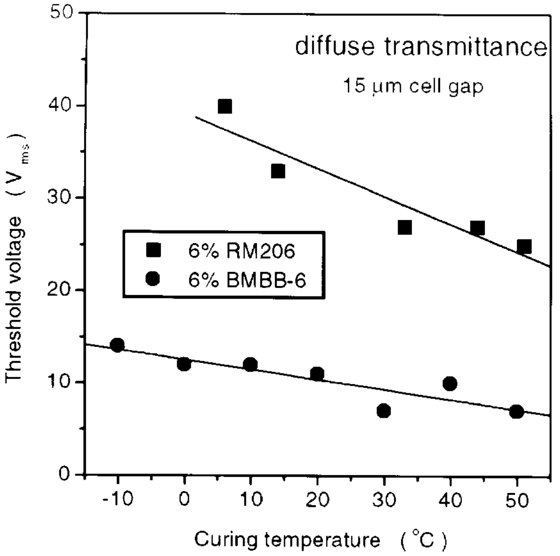

Figure 8. Dependence of the threshold voltage of the diffuse transmittance on curing temperature for the planar to focal-conic texture transition for 6 wt % RM206 (■) and 6 wt % BMBB-6 (●) polymer networks.

times increase significantly as the curing temperature is raised [figure 9 (*a*) and (*b*), open symbols]. These behaviours are reasonable since in both instances the rise times represent an electric field driven reorientation, while the decay times result from an elastically driven, and thus polymer influenced, reorientation.

4. Discussion

The data presented above show that the trends in electro-optical performance which are observed as the curing temperature of a PSCT system is increased are the same as those observed as the concentration of the polymer network is decreased. As the curing temperature is increased, the diffuse reflectivity decreases, the diffuse transmittance increases, and the threshold voltages for both diffuse reflectivity and transmittance decrease. These same trends are all observed for decreasing polymer content [5]. Further, as the curing temperature of RM206 PSCTs is increased, a transition from one- to

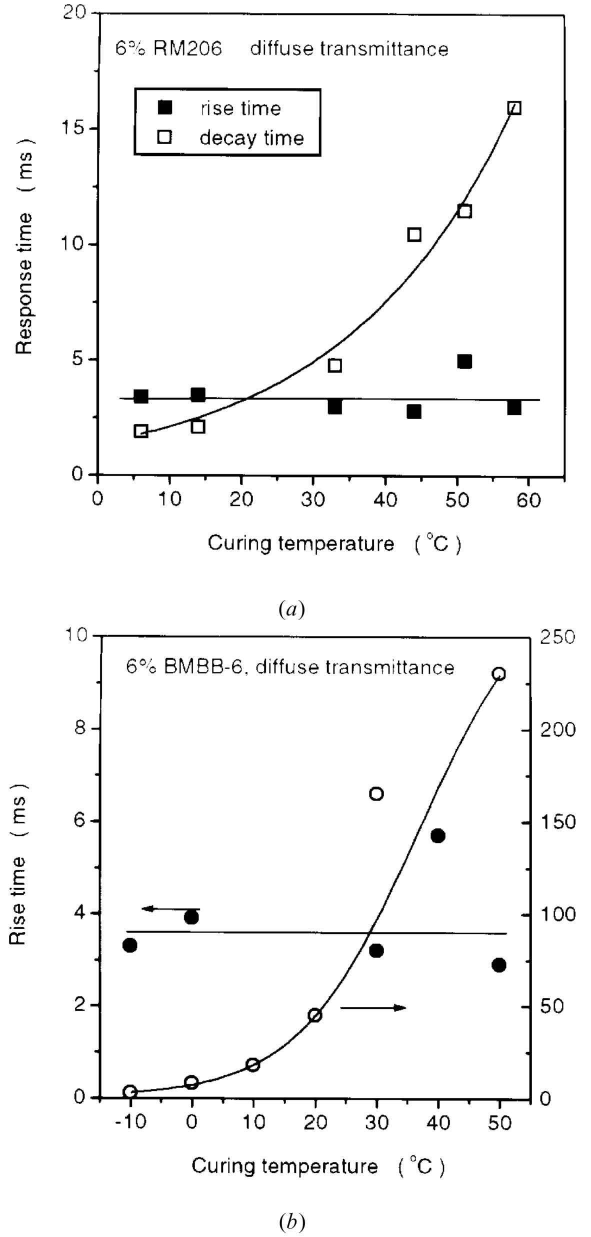

(*a*)

(*b*)

Figure 9. Dependence of the response times of the diffuse transmittance on curing temperature for the planar to focal-conic texture transition for (*a*) 6 wt % RM206 (■) and (*b*) 6 wt % BMBB-6 (●) polymer networks. Rise times are shown with closed symbols and decay times with open symbols.

two-stage switching, similar to that observed for decreasing RM206 content, is observed. For the case of varying polymer concentration, it was shown that the lower concentrations of polymer resulted in larger voids within the polymer network. This, in turn, resulted in larger regions of 'bulk-like' liquid crystalline material. It was argued that the presence of both 'bulk-like' and polymer dominated regions of liquid crystalline material resulted in the observed two-stage switching. The present data are consistent with this model provided that increasing the curing temperature of a PSCT cell results in larger voids within the polymer network.

Figure 10 (*a*)–(*d*) show SEM images of 6 wt % RM206 PSCT polymer networks which have been UV cured at 14, 33, 44 and 51°C, respectively. From these images it is clear that the mean void size within these networks does indeed increase with curing temperature. Most notably, figure 10 (*c*) and (*d*) reveal much larger voids than do 10 (*a*) and (*b*). In figure 11 SEM images are shown of 6 wt % BMBB-6 PSCT polymer networks which have been UV cured at −10, 0, 20, and 40°C, respectively. In these images there is no obvious correlation between curing temperature and network void size. In as much as the BMBB-6 cells exhibited significantly less change in electro-optic properties as a function of curing temperature, this is not surprising. In general, compared with the RM206 structures, the BMBB-6 networks are coarser for all curing temperatures. This allows a larger fraction of the liquid crystal to experience a more bulk-like environment and is consistent with the observation of lower voltage thresholds, as well as two-stage switching in all of the BMBB-6 samples studied.

The networks shown in figures 10 (*b*)–(*c*) and 11 (*a*)–(*d*) were taken from PSCT cells which exhibited two-stage switching, whereas those shown in figure 10 (*a*) and (*b*) exhibited single-stage switching. As expected, the cells exhibiting two-stage switching have significantly larger network voids. Based on estimates from the 6 wt % RM206 SEM data, we find that an average void size of 0·4–0·5 μm is observed near the transition from one- to two-stage switching. It is noteworthy that the observation of voids of this size within the network is correlated with the observation of the onset of two-stage switching as the concentration, curing intensity, or UV dose is varied as well. We also find that the helical structure of the cholesteric has been more clearly transferred to the polymer network in cells which exhibit only single-stage switching.

A comparison of the diffuse reflectivity (figure 1) and diffuse transmittance (figure 6) data allows for an identification of the different regions which contribute to forward and back scattering. The diffuse transmittance, or fraction of forward scattered light, shows an increase at low voltages and no two-stage switching. Decreasing the curing temperature, and thus increasing the polymer/liquid crystal interfacial area (figure 10), results in a decrease of the diffuse transmittance (figure 8). This suggests that those regions of liquid crystal material which are only slightly influenced by the polymer network contribute mainly to the forward scattering. In contrast, the diffuse reflectivity (which describes the fraction of light being back scattered) exhibits increasing

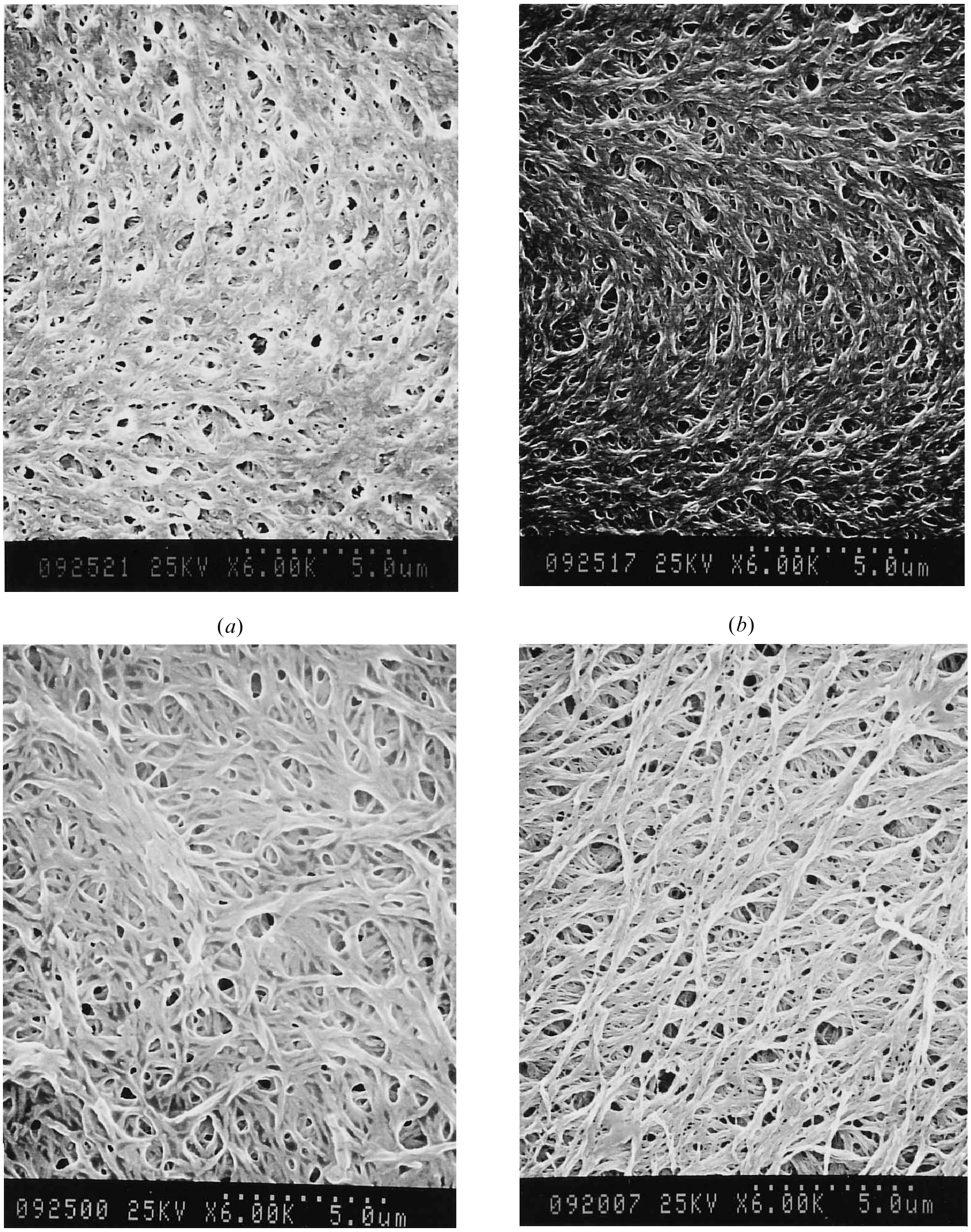

(*a*) (*b*)

(*c*) (*d*)

Figure 10. SEM photographs of the polymer network structure of 6 wt % RM206 formed at different curing temperatures: (*a*) 14°C, (*b*) 33°C, (*c*) 44°C and (*d*) 51°C. The dimensions of the regions shown are $14{\cdot}4 \times 17{\cdot}2\,\mu m^2$.

values for decreasing curing temperature, indicating that those liquid crystal regions which are strongly dominated by the network structure contribute primarily to the back scattering. This is consistent with scattering theory, which predicts increased back scattering as the size of the scattering objects, in this case the focal-conic domains, decreases towards the wavelength of the incident light. As the scattering objects become increasingly larger than the incident wavelength, forward scattering becomes favoured. If the polymer dominated liquid crystal material is characterized by smaller average focal-conic domain sizes than are observed for bulk-like material, this would account for the relative intensities of forward and back scattering observed with increasing network density.

The structures of the RM206 and BMBB-6 PSCT networks shown in figures 10 and 11 are fundamentally different. For all curing temperatures, the RM206

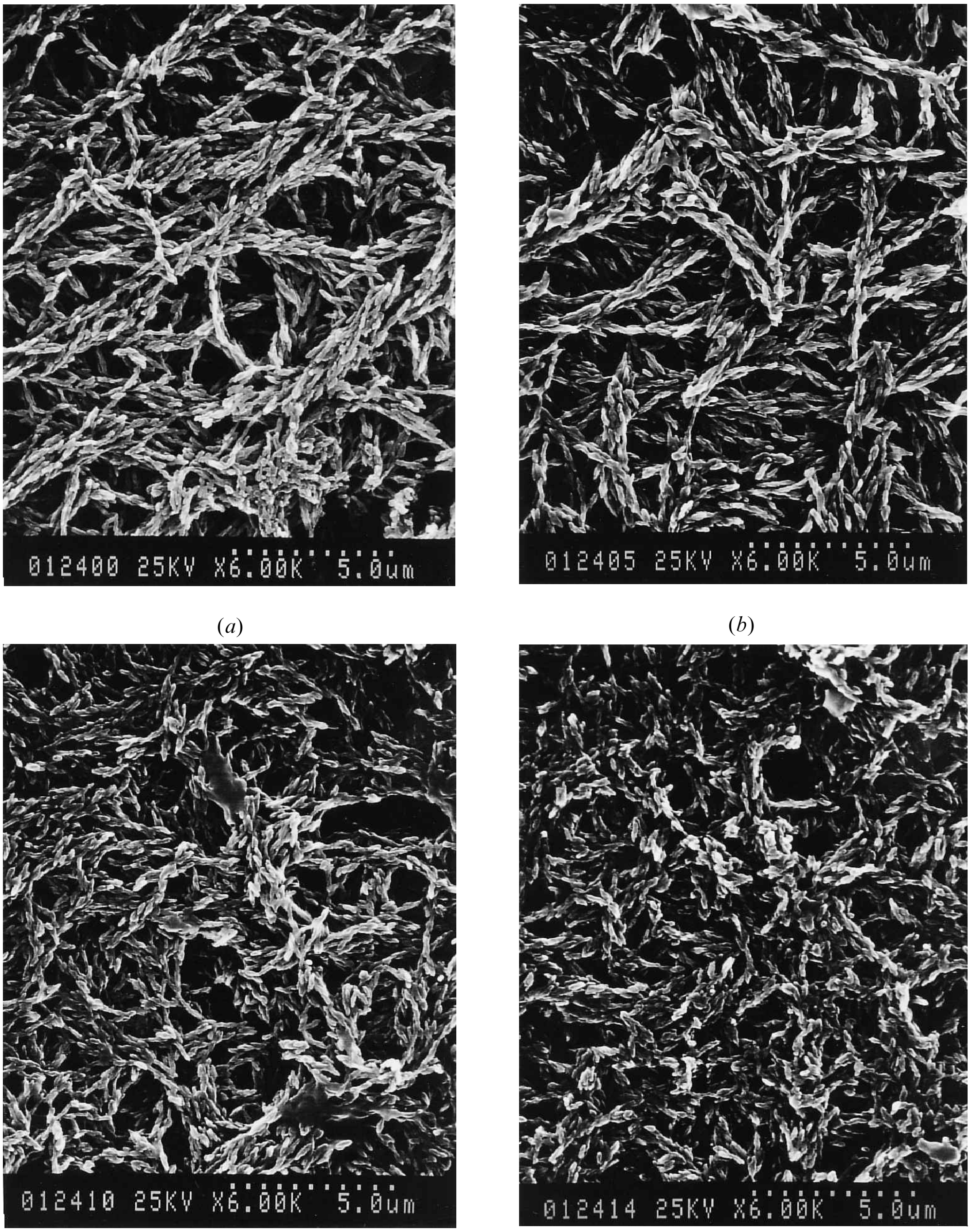

(*a*) (*b*)

(*c*) (*d*)

Figure 11. SEM photographs of the polymer network structure of 6 wt % BMBB-6 formed at different curing temperatures: (*a*) -10°C, (*b*) 0°C, (*c*) 20°C and (*d*) 40°C. The dimensions of the regions shown are $14{\cdot}4 \times 17{\cdot}2\,\mu m^2$.

networks consist of a highly interconnected, tight network of fine polymer fibres. In contrast, the strands in the BMBB-6 network are thicker and appear to be composed of individual 'rice-grain-like' particles with dimensions between 0·2 and 1 μm. Over the temperature range studied (-10–60°C), the morphologies of the BMBB-6 and RM206 networks remained fundamentally different. These results suggest that the temperature of the polymerization process does not determine the fundamental morphology of the polymer strands, it simply affects the size of the polymer voids; that is, it affects the spacing between strands.

For PSCT polymer networks composed of discrete particles, such as the BMBB-6 networks shown in figure 11, Rajaram *et al.* [7] have suggested that the size of the discrete particles is determined by a cross-over from reaction limited to diffusion limited growth. Their model predicts that the particle size should scale as absolute temperature to the one-third power. Over the temperature range we have studied, this would correspond to a change in size of about 8%. Our SEM data do not allow the observation of changes this small; variations of this magnitude would be lost within the fluctuations between different regions. Also, we note that while Rajaram *et al.* reported changes in the morphology of BABB-6 PSCT networks as the curing temperature was varied, they associated these changes with a transition to the smectic state within the monomer. As we have not passed through any such transitions in these studies, it is not surprising that no such morphological changes were seen.

5. Conclusions

We have studied the effect of curing temperature on the electro-optical and morphological properties of PSCTs. In general, higher curing temperatures result in polymer networks characterized by larger average mesh sizes. However, variation in temperature over the range studied has no significant impact on the morphology of the polymer strands. This is true despite the fact that different monomers result in radically different polymer morphologies.

The transition from one- to two-stage switching in 6 wt % RM206 as the curing temperature is increased is consistent with our previously discussed model [5]. The higher curing temperatures result in polymer networks with larger voids. This, in turn, results in large regions of liquid crystal which are only slightly influenced by the network, thus accounting for the two-stage switching, low thresholds and long decay times. Decreasing the curing temperature results in a formation of polymer network structures with smaller average mesh sizes in which a single-process reorientation is observed, as well as higher threshold voltages and faster decay times. This follows from the fact that in all regions the liquid crystal material is strongly dominated by the network.

References

[1] For a review see *Liquid Crystals in Complex Geometries*, 1996, edited by G. P. Crawford and S. Žumer (London: Taylor and Francis).

[2] For a review see *Liquid Crystal Dispersions*, 1995, P. S. Drzaic (Singapore: World Scientific).

[3] Broer, D. J., Gossink, R. G., and Hikmet, R. A. M. 1990, *Angew. makromol. Chem.*, **183,** 45; Hikmet, R. A. M., and Zwerver, B. H., 1991, *Mol. Cryst. liq. Cryst.*, **200,** 197; Hikmet, R. A. M., and Zwerver, B. H., 1992, *Liq. Cryst.*, **12,** 319; Hikmet, R. A. M., and Zwerver, B. H., 1993, *Liq. Cryst.*, **13,** 561; Hikmet, R. A. M., Chap. 3 of [1].

[4] Yang, D.-K., Chien, L.-C., and Doane, J. W., 1992, *Appl. Phys. Lett.*, **60,** 3102; Yang, D.-K., West, J. L., Chien, L.-C., and Doane, J. W., 1994, *J. Appl. Phys.*, **76,** 1331 (1994); Yang, D.-K., Chien, L.-C., and Fung, Y. K., Chap. 5 of [1].

[5] Dierking, I., Kosbar, L. L., Afzali-Ardakani, A., Lowe, A. C., and Held, G. A., 1997, *J. appl. Phys.*, **81,** 3007.

[6] Boutellier, L., LeBarny, P., Rubin, P., and Dubois, J. C., 1994, in Proceedings of the 14th International Displays Research Conference, Monterey, CA, p. 195.

[7] Rajaram, C. V., Hudson, S. D., and Chien, L.-C., 1996, *Chem. Mater.*, **8,** 2451.